

Molecular-dynamics study of supercooled *ortho*-terphenyl

Laurent J. Lewis\*

*Département de Physique et Groupe de Recherche en Physique et Technologie des Couches Minces, Université de Montréal,  
Case Postale 6128, Succursale A, Montréal, Québec, Canada H3C 3J7*

Göran Wahnström†

*Department of Applied Physics, Chalmers University of Technology and University of Göteborg,  
S-412 96 Göteborg, Sweden*

(Received 21 October 1993; revised manuscript received 28 July 1994)

We present the results of a detailed molecular-dynamics study of relaxation in the van der Waals system *ortho*-terphenyl in the supercooled regime. The molecule is described by a simple rigid three-site model, with interactions between different molecules of the Lennard-Jones form. We find that the long-time ( $\alpha$ ) relaxation, as determined from the intermediate scattering function, is well described by a Kohlrausch law. The zero-time amplitude of this process, often referred to as the “nonergodicity parameter,” which can be interpreted as a Debye-Waller factor, is seen to depart from a linear temperature dependence and seems to exhibit a “singularity” at a temperature substantially larger than the conventional glass transition temperature, in accord with neutron-scattering data, and as predicted by mode-coupling theory. We find that the observed anharmonic behavior around  $T_c$ , as well as the decay of the scattering functions, is equally evident from both orientational and translational correlations. The latter observation indicates that the structural changes that take place during  $\alpha$  relaxation are neither specifically orientational nor specifically translational. Investigation of the van-Hove self-correlation for both center-of-mass and orientational motion reveals the existence of a strong non-Gaussian spatial dependence at intermediate times and of processes, even at low temperatures, that cannot be described as simple vibrational motion, and which consist of rapid reorientations of the molecules about their essentially frozen centers of mass. This motion may be related to the fast secondary mode seen in experiments.

PACS number(s): 61.20.Lc, 64.70.Pf, 61.43.Fs, 61.20.Ja

## I. INTRODUCTION

It is a fundamental problem of condensed-matter physics to determine whether there is a real phase transition that leads a liquid into a glass at a temperature near the experimentally defined (calorimetric) transition point  $T_g$  [1]. Early theories of the “glass transition” postulate that a real transition will take place if the cooling rate is infinitely slow [2], which puts the critical temperature below the calorimetric  $T_g$ . The recent mode-coupling theory (MCT) [3,4], in contrast, predicts the existence of a dynamical instability at a temperature somewhat above  $T_g$ , by perhaps 30–150 K.

The central idea behind the MCT is that density fluctuations  $\delta\rho(q, t)$  couple nonlinearly with one another; the dynamical feedback that results leads, upon lowering the temperature (or increasing the density), to a progressive slow down of the decay in time of the fluctuations, until they are completely frozen out at the critical, or “crossover,” temperature  $T_c$ . The relaxation mode associated with this slow-down process is referred to as primary or  $\alpha$  relaxation, and in turn leads to an increase

of the viscosity upon approaching  $T_c$ . In its idealized version, therefore, the glass transition in the MCT is an ergodic to nonergodic transition. This theory, however, which leads to a sharp transition at  $T_c$ , neglects some processes, often referred to as “thermally activated hopping processes,” and overestimates the “rigidity” of the cage around each particle formed by its neighbors. More recent versions of the theory [5–7] incorporate additional nonlinearities in order to account for those processes, which results in the transition being smeared out.

One of the most extensively studied glass-forming systems is *ortho*-terphenyl (1,2-diphenylbenzene), a nonpolar organic liquid. It is a so-called “fragile” glass former (in contrast to “strong” or network-forming liquids, to use Angell’s nomenclature — Ref. [8]). It consists of well-defined molecular units (three connected benzene rings); the intermolecular interaction is of the short-range van der Waals (Lennard-Jones) type and it shows little tendency to crystallization, with a melting temperature  $T_m$  of 329 K. The system can easily be supercooled and the viscosity increases by 10 orders of magnitude in the small temperature range between 295 and  $T_g = 243$  K [9].

Several years ago Johari and Goldstein [10], and more recently Wu and Nagel [11], using dielectric measurements, have identified a secondary, or  $\beta$ , process in *o*-terphenyl, at kHz frequencies, in the temperature range 200–240 K, the temperature dependence of which be-

\*Electronic address: lewis@physcn.umontreal.ca

†Electronic address: wahnstrom@fy.chalmers.se

ing Arrhenius-like. Inelastic neutron-scattering measurements have been performed also, clearly demonstrating the existence of a *fast* secondary process, on the *picosecond* time scale, giving rise to an anomalous decrease of the Debye-Waller factor at temperatures close to 290 K [12–15]. A most interesting observation is that at temperatures below 290 K, rotational and translational motion “decouple” [16]. Depolarized light scattering experiments also reveal the existence of a fast process, with an essentially temperature-independent correlation time (of about 3 ps) in the temperature range 250–450 K [17]. Finally, by using nuclear magnetic resonance measurements, a fast local process has been observed in the glassy state [18]. The dynamic anomalies found around 290 K have been interpreted in terms of the MCT, and this temperature has been associated with  $T_c$ , the “critical” or crossover temperature in the MCT. Very recently, Steffen *et al.* [19] have found that their depolarized light scattering data could be made compatible with the predictions of MCT with this value of  $T_c$ .

Motivated by these experimental observations, and in an attempt to better understand the atomic-scale processes that take place on the ps time scale in supercooled liquids, we have performed an extensive series of molecular-dynamics (MD) simulations [20] of a model that, as we will see, accounts well for several properties of *o*-terphenyl [21–23]. Despite its simplistic nature, the model appears to contain some of the essential physics of the real material, and our calculations, therefore, are of relevance to laboratory glass-forming systems. We note also that MD is well suited to probe mesoscopic time scale since runs, with some effort, can extend to times of the order of ns.

Several computer simulations have been performed in the past on simple atomic systems [24], and in particular on two-component mixtures in order to bypass crystallization. Atomic systems, however, exhibit cooperative jump-diffusive motion at low temperatures, which influences markedly the dynamics even for times shorter than 1 ns [25,26]. Since it is believed that such processes are not well accounted for by the idealized version of the MCT, we find it important to examine a system where they are likely to be rare. The present system of non- (but quasi-) spherical molecules achieves this, as we will see in detail below.

We note that corresponding studies on molecular systems have been carried out by Signorini *et al.* on the ionic glass  $[\text{Ca}(\text{NO}_3)_2]_{0.4}[\text{KNO}_3]_{0.6}$  [27], and by Sindzinger and Klein [28] and Alonso *et al.* [29] on methanol.

As discussed in detail below, we find that our simple model reproduces well the anomalous decrease of the Debye-Waller factor seen in inelastic neutron-scattering experiments [12] near  $T_c$ , which also correlates well with the temperature dependence of the nonergodicity parameter predicted by the MCT. We find that the observed anharmonic behavior around  $T_c$ , as well as the decay of the scattering functions, is equally characteristic of orientational and translational motion. Investigation of the van-Hove self-correlation for both center-of-mass and orientational motion reveals the existence of a strong non-Gaussian spatial dependence at intermediate times. At

low temperatures, we detect processes that cannot be described as simple vibrational motion, and which consist of rapid reorientations of the molecules about their essentially frozen centers of mass.

Our paper is organized as follows: In Sec. II, we present the details of our model, and give a summary of the runs performed. The results are presented and discussed in Sec. III. We start with the thermodynamic properties, which we use to establish that the system is in a “good” glassy state. We present next our results for the pair distribution functions and static structure factors. We move on to a discussion of dynamic properties, including diffusion coefficients and various correlation functions. We describe in detail our results for the intermediate scattering function, both the incoherent and the coherent contributions; we also distinguish between self-contributions, and those contributions associated with the motion of the centers of mass, as well as of the orientations. Section III ends with a discussion of diffusion, as deduced from the real-time–real-space van-Hove correlation function; we will comment there on the anharmonic behavior of the *o*-terphenyl molecules in the supercooled regime, and also examine time-dependent orientational distribution functions. Section IV summarizes our results.

## II. MODEL AND COMPUTATIONAL DETAILS

In order to properly account for the slow relaxation processes in the supercooled regime, it is important that runs be sufficiently long at every temperature, and in particular at low temperatures, since dynamical processes slow down dramatically upon cooling. This is however a serious problem for molecular-dynamics simulations: denoting by  $\tau$  the temperature-dependent relaxation time characteristic of the (slow) dynamics of the liquid in the supercooled state, there necessarily comes a point where  $\tau$  becomes larger than the largest practical simulation time (of the order of ns). A compromise has to be established, therefore, between system size, run times, and the complexity of the model.

In view of the above remark, the following simple model for *o*-terphenyl was developed and employed: The *o*-terphenyl molecule was represented by a three-site complex, each site playing the role of a whole benzene ring. For the position of site  $a$  ( $a = 1, 2, \text{ or } 3$ ) in molecule  $i$ , with  $i = 1, \dots, N$  ( $N$  is the total number of molecules), we write

$$\mathbf{R}_{i,a} = \mathbf{R}_i^{\text{c.m.}} + \mathbf{u}_{i,a} \quad (2.1)$$

where  $\mathbf{R}_i^{\text{c.m.}}$  denotes the location of the center of mass of molecule  $i$ . Molecules were chosen to interact with one another pairwise additively, i.e., by virtue of the site-site approximation. The interaction between two sites on different molecules was taken to be of the Lennard-Jones form,  $v(r) = 4\epsilon[(\sigma/r)^{12} - (\sigma/r)^6]$ , since van der Waals interactions are known to be the dominant interaction in this system. The rigid-molecule approximation was invoked in order to simplify the calculations, i.e., we neglected the molecules internal degrees of freedom, a very reasonable assumption in the present context

[13,30]. Each molecule, therefore, was assigned a fixed bond length, chosen equal to  $\sigma$ , the Lennard-Jones “hard-sphere diameter” (the actual numerical value is discussed below), and a fixed bond angle, here taken to be  $75^\circ$ . The latter value is approximate, but the real molecule suffers some “torsioning” [31,32]; further, this choice (rather than  $60^\circ$ ) makes the molecule slightly asymmetric. Explicit values for the potential parameters  $\epsilon$  and  $\sigma$  were determined by carrying out some test runs in the liquid phase, calculating the molar volume and the diffusion coefficient, and adjusting to the corresponding experimental numbers at  $T = 400$  K [ $v = 0.2308$  m<sup>3</sup> kmol<sup>-1</sup> (Ref. [33]) and  $D = 60.0 \times 10^{-7}$  cm<sup>2</sup> s<sup>-1</sup> (Ref. [34])]. We obtain, in this way,  $\epsilon/k_B = 600$  K and  $\sigma = 4.83$  Å.

The simulation box, chosen to be cubic, contained  $N = 324$  molecules (972 sites) and periodic boundary conditions were employed in all three directions to eliminate surface effects. Size effects were assessed by performing runs on both a smaller (108 molecules) and a larger (2592 molecules) system, as will be discussed in Sec. IIID 2. The equations of motion were solved using a standard fourth-order Gear predictor-corrector algorithm for the translational degrees of freedom, and a 5th-order Gear algorithm for the orientational coordinates, expressed here in terms of quaternions. A time step of 7 fs was found to conserve energy adequately, and, therefore, used in all runs except one (labeled E — cf. Table I) where 5 fs was used.

Starting with a high-temperature liquid, the system was cooled through the glass transition at a rate determined by the (temperature-dependent) relaxation time  $\tau$  for  $\alpha$  processes discussed above. A total of 14 different temperatures were investigated (including a “disordering run” at 510 K — near the boiling point of *o*-terphenyl — which we will ignore in future discussions). At each temperature, the system was first equilibrated for a period of time as long as  $\tau$  at high temperatures, and as long as possible at lower temperatures. As we will see in the next section, the system falls out of equilibrium at a temperature of about 250 K: it is no longer possible to afford “long” runs beyond that point. During equi-

libration, the simulation was performed in the isothermal-isobaric ( $N, P, T$ ) ensemble using the constant-pressure algorithm of Andersen in order to determine the size of the MD cell (the external pressure was set to 1 bar). Following equilibration, “production runs” were carried out in the microcanonical ( $N, V, E$ ) ensemble, during which statistics were accumulated and trajectories saved for a *posteriori* treatment, including the calculation of various correlation functions of interest.

Information pertinent to each run is given in Table I. This includes the temperature  $T$ , the potential energy  $E_{\text{pot}}$ , the calculated internal pressure  $P$  in the constant-volume portion of the run, the molar volume  $v$ , the diffusion coefficient  $D_{\text{c.m.}}$  for center-of-mass motion (as estimated from a calculation of the mean-square displacements; see Sec. IIIC) for those temperatures at which it could be safely determined, and the equilibration and total run times  $t_{\text{equil}}$  and  $t_{\text{max}}$  at each temperature. In one case, run C, we had problems to achieve a stable situation, which is apparent in the somewhat large and negative value of the internal pressure. This run, therefore, will have to be treated with care in the analysis of the data. We will return, in the course of later discussion, to some of the quantities presented in Table I.

### III. RESULTS AND DISCUSSION

#### A. Thermodynamic properties

The evolution in temperature of various macroscopic, time-averaged quantities are listed in Table I. Figures 1 and 2 show the variations of the molar volume  $v$  and the total energy  $E_{\text{tot}}$ , respectively, with temperature. The experimental values of the melting temperature and the calorimetric glass transition temperature are, we recall,  $T_m = 329$  K and  $T_g = 243$  K, respectively. As we will see later, the “critical temperature” — in the sense of MCT — is located near  $T_c = 280$  K in our model. From Figs. 1 and 2, we see that at about 250 K the temperature dependence of both volume and energy changes slope. This re-

TABLE I. Evolution in temperature of the simulation. For each run, we list the average temperature  $T$ , the potential energy  $E_{\text{pot}}$ , the internal pressure  $P$  during the constant-volume (production) portion of the run (the external pressure is set to 1 bar), the molar volume  $v$ , the diffusion coefficient for centers of mass  $D_{\text{c.m.}}$ , the equilibration time  $t_{\text{equil}}$ , and the maximum simulation time  $t_{\text{max}}$  (including the constant-pressure equilibration).

Run	$T$ (K)	$E_{\text{pot}}$ (kJ mol <sup>-1</sup> )	$P$ (kbar)	$v$ (m <sup>3</sup> kmol <sup>-1</sup> )	$D_{\text{c.m.}}$ ( $10^{-7}$ cm <sup>2</sup> s <sup>-1</sup> )	$t_{\text{equil}}$ (ns)	$t_{\text{max}}$ (ns)
A	400	-67.771	-0.012	0.2303	57	0.200	0.500
B	346	-71.536	+0.028	0.2225	19	0.322	0.882
C	318	-72.959	-0.136	0.2206	13	0.315	0.980
D	305	-74.613	+0.016	0.2169	3.3	0.385	1.295
E	291	-75.337	-0.030	0.2161	1.9	0.850	2.050
F	281	-75.695	-0.017	0.2153	1.5	0.490	1.400
G	275	-76.328	+0.004	0.2140	0.7	0.560	1.610
H	266	-76.885	-0.044	0.2136		0.980	2.100
I	255	-77.363	+0.005	0.2122		0.840	1.960
J	205	-78.923	+0.020	0.2096		0.490	1.610
K	173	-79.890	+0.018	0.2082		0.420	0.630
L	133	-81.050	-0.025	0.2067		0.420	0.630
M	101	-81.962	-0.032	0.2053		0.490	0.700

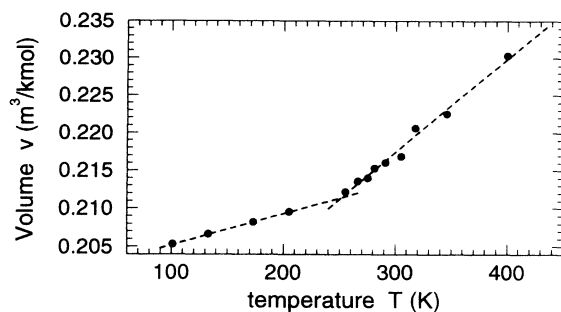


FIG. 1. Molar volume as a function of temperature. The dashed lines are guides to the eye.

fects the fact that the system is falling out of equilibrium, i.e., it is no longer possible for it to equilibrate properly in the time window used in the simulation (see Table I). We expect our simulations, therefore, to provide an adequate description of the relaxational dynamics only at temperatures above 250 K, and in particular close to  $T_c$ , where interesting effects are expected. Below 250 K the system is nonergodic and proper equilibration cannot be achieved. In a previous simulation [26], however, it was demonstrated on the basis of three independent sets of calculations, that the low-temperature vibrational properties are relatively insensitive to the cooling procedure.

We have observed no change in the thermodynamic properties during the cooling process which could indicate a tendency for crystallization, a problem which has to be dealt with in laboratory experiments. The numerical value we find here for the density in the supercooled state is quite similar to the value found experimentally [0.2059 and 0.2095  $\text{m}^3 \text{kmol}^{-1}$  at 250 and 273 K, respectively (Ref. [9])], and substantially larger than that appropriate to the crystalline phase of *o*-terphenyl [0.1978 and 0.1987  $\text{m}^3 \text{kmol}^{-1}$  at 303 and 326 K, respectively (Ref. [33])], which further asserts that the system is in a “good” glassy state.

### B. Pair distribution functions

The radial pair distribution functions for centers of mass  $g_{c.m.}(r)$ , and for sites  $g(r)$ , are displayed in Fig. 3 at two temperatures, namely 400 K (well into the liq-

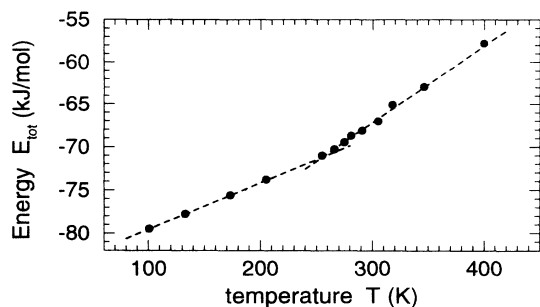


FIG. 2. Total energy as a function of temperature. The dashed lines are guides to the eye.

uid phase) and 266 K (well into the supercooled phase).  $g_{c.m.}(r)$  is rather featureless at medium and long range, as expected for a liquid or a glass, but shows some structure at short range: the short- $r$  side of the first peak displays a weak shoulder at high temperature, which turns into a peak at low temperature. The distribution for sites, on the other hand, exhibits pronounced oscillations caused by our use of a rigid molecule, but is nevertheless typical of amorphous systems.

The Fourier transform of the pair distribution function is the static structure factor, obtained experimentally by diffraction experiments. This quantity is shown in Fig. 4, both for diffraction by centers of mass,  $S_{c.m.}(q)$ , and by sites  $S(q)$  for the same two temperatures as the above pair distribution functions. (We have evaluated the static structure factors directly in reciprocal space to avoid the cutoff problems inherent to Fourier transforms.) In the case of *o*-terphenyl, the neutrons are predominantly scattered by the hydrogens, which corresponds most closely to scattering by the “sites” in our model, as opposed to the centers of mass. We find  $S(q)$  for sites to exhibit a smooth behavior typical of disordered (liquid or glassy)

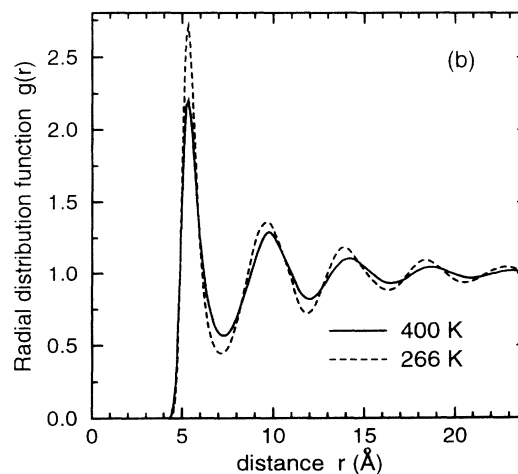
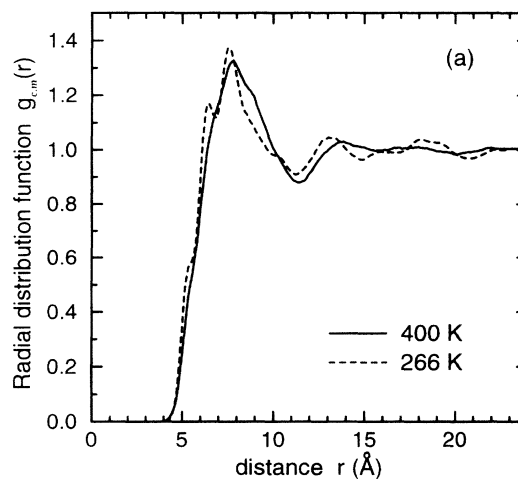


FIG. 3. (a) Radial distribution function for centers of mass,  $g_{c.m.}(r)$ , at 400 K (full line) and 266 K (dashed line). (b) Same thing for sites,  $g(r)$ .

systems, with a relatively sharp first peak at about  $1.5 \text{ \AA}^{-1}$ , whose intensity increases upon cooling. The static structure factor of *o*-terphenyl has been measured recently by Bartsch *et al.* using neutron scattering [35]. In contrast to our results, they find that the first peak is split, with maxima at  $1.4$  and  $1.9 \text{ \AA}^{-1}$ . The temperature dependence of  $S(q)$  was also investigated in this study: It was observed that the intensity of the first subpeak, at  $1.4 \text{ \AA}^{-1}$ , is essentially independent of temperature, while the intensity of the  $1.9 \text{ \AA}^{-1}$  subpeak increases upon cooling, in a continuous (approximately linear) manner. The second subpeak, therefore, is not related to the dynamical anomalies predicted by MCT at the glass transition (nor is, of course, the  $T$ -independent first subpeak). Bartsch *et al.* also conclude, from their experiment, that the changes in the second subpeak intensity with temperature correspond to changes in the short-range ( $\sim 10$ – $15 \text{ \AA}$ ) intermolecular structure, while the intramolecular structure depends very little on temperature.

Our model for *o*-terphenyl, as the above comparison to structure factor measurements demonstrate, gives only an approximate description of the static intermolecular

structure (and provides no information about the intramolecular structure). The aim of the present study, however, is to investigate the dynamics of relaxation. In view of the conclusion by Bartsch *et al.* that the temperature dependence of the intermolecular structure is *not* related to the dynamic anomalies predicted by MCT, we expect that the deficiencies of our model will be of little consequence in the study of the dynamic behavior of *o*-terphenyl. An interesting extension of the present work, evidently, would be to include all hydrogen particles as well as the tilt angle between the benzene rings in our three-body model, in order to understand the details of the intermolecular structure.

### C. Diffusion coefficient

We have determined the diffusion coefficients at several temperatures by taking the slope of the long-time limit of the mean-square displacements,  $D_{c.m.} = \lim_{t \rightarrow \infty} \langle |\mathbf{R}_i^{c.m.}(t) - \mathbf{R}_i^{c.m.}(0)|^2 \rangle / 6t$  [23]. The results are given in Table I. The diffusion constant drops rapidly upon cooling, and there comes a point in temperature, here about  $266 \text{ K}$ , where it is no longer possible (because of statistical inaccuracies) to extract meaningful values from the long-time behavior of the mean-square displacements. The corresponding (high-temperature) experimental numbers [34] are  $60 \times 10^{-7} \text{ cm}^2 \text{ s}^{-1}$  at  $400 \text{ K}$  — a value we used to fit the parameters of our model — and  $22 \times 10^{-7} \text{ cm}^2 \text{ s}^{-1}$  at  $363 \text{ K}$ , in line with our results. In Sec. III E we will study the diffusive motion in more detail by considering the self-part of the van-Hove correlation function.

### D. Intermediate scattering function

Direct information on relaxation processes in the liquid and supercooled (glassy) phases is provided by the real-time density-density correlation function, or “intermediate scattering function” [36],

$$F(\mathbf{q}, t) = \frac{1}{3N} \left\langle \sum_{i,j=1}^N \sum_{a,b=1}^3 \exp[i\mathbf{q} \cdot (\mathbf{R}_{i,a}(t) - \mathbf{R}_{j,b}(0))] \right\rangle. \quad (3.1)$$

Here,  $\mathbf{R}_{i,a}(t)$  denotes the position of “site”  $a$  in molecule  $i$  at time  $t$  [cf. Eq. (2.1)]. For an essentially isotropic material like a liquid or a glass, the angular dependence vanishes, i.e.,  $F(\mathbf{q}, t) \equiv F(q, t)$ . This function is of utmost interest since it is available from inelastic neutron-scattering experiments by an inverse Fourier transform of the dynamic structure factor,  $S(q, \omega)$ .

#### 1. Self-correlations for sites

The neutrons essentially see only the hydrogens in *o*-terphenyl, and the scattering is incoherent, i.e., it is the *self*-part  $S^s(q, \omega)$  [or equivalently  $F^s(q, t)$ ] which is mea-

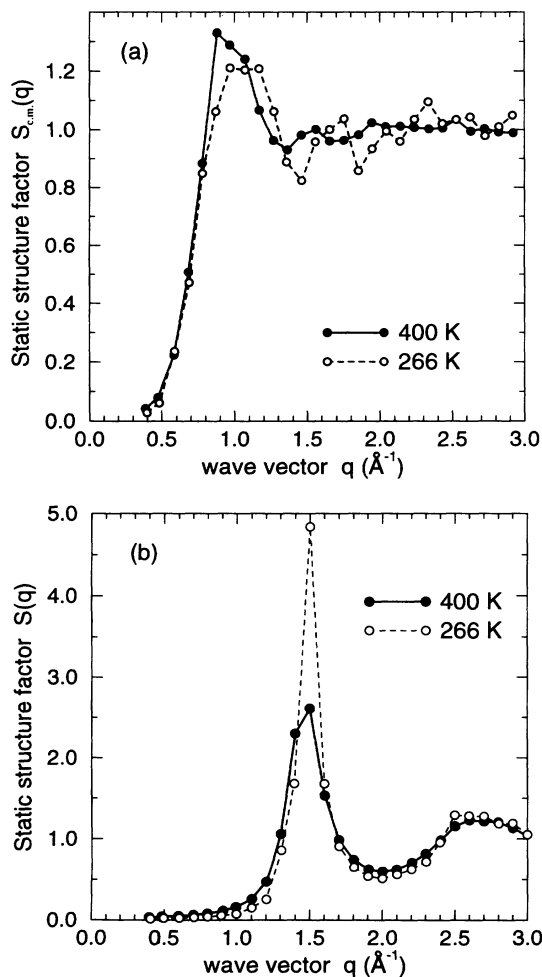


FIG. 4. (a) Static structure factor for centers of mass,  $S_{c.m.}(q)$ , at  $400 \text{ K}$  (full line and closed circles) and  $266 \text{ K}$  (dashed line and open circles). (b) Same thing for sites,  $S(q)$ .

sured, corresponding most closely to scattering by the sites here. We have calculated this function [by retaining only terms with  $i = j$  and  $a = b$  in Eq. (3.1)] for several wave vectors, and in particular for values of  $q$  close to the ones investigated by Bartsch *et al.* by neutron scattering [12]. We show in Fig. 5 the results for two specific wave vectors, namely  $q = 1.35$  and  $1.94 \text{ \AA}^{-1}$  [i.e., near the first maximum of the static structure factor and at the minimum which follows — see Fig. 4(b)], at several temperatures through the glass transition.

As evident from Fig. 5, density-density correlations are short-lived in the high-temperature liquid, and  $F^s(q, t)$  decays rapidly. When temperature is lowered, however, relaxation slows down dramatically (note the logarithmic time scale) and pronounced stretching is observed. This slow (long-time) decay corresponds to  $\alpha$  relaxation. At  $T = 266$  and  $255 \text{ K}$  (the latter is not shown), signs that such relaxation processes are still taking place are visible; for temperatures beyond this point, however,  $F^s(q, t)$  exhibits no decay — except for the initial microscopic re-

laxation — for times less than  $10^{-9}$  s, corresponding to the time window accessible in our simulations: thus, the system is “structurally arrested” on this time scale.

As other studies — either numerical or experimental — demonstrate, the slow  $\alpha$  process is well fitted by a stretched exponential, or Kohlrausch-Williams-Watts (KWW) law,

$$f_{\text{KWW}}(q, t) = a \exp[-(t/\tau)^\beta], \quad (3.2)$$

where  $\tau$  is a relaxation time,  $0 < \beta < 1$  is the stretching exponent, and  $a$  is the amplitude. We have performed, for each wave vector, and at each temperature at which it was possible, a nonlinear least-squares fit of  $F^s(q, t)$  to the KWW law. We have allowed all three parameters  $a$ ,  $\beta$ , and  $\tau$ , to vary independently, and they were assumed to depend on both temperature and wave vector.

Since the stretched exponential only describes the *long* time behavior, a time window  $t_1 < t < t_2$  has to be chosen over which the fit is done. The upper limit,  $t_2$ , was determined simply by the time extension of the MD simulation, taking care to avoid the statistically poor region of the function near maximum time. The choice of lower limit  $t_1$  on the other hand, is a source of concern, and results in some uncertainty on the fitted parameters. Using  $t_1 = 3 \text{ ps}$ , we obtain  $[a, \beta, \tau] = [0.559, 0.69, 0.317 \text{ ns}]$  for run G with  $q = 1.94 \text{ \AA}^{-1}$ , which can be compared with the result for  $t_1 = 10 \text{ ps}$ ,  $[0.533, 0.77, 0.340 \text{ ns}]$ . The fit is slightly better using  $t_1 = 10 \text{ ps}$ . We adopted this value, therefore, and in order to bias the fit as little as possible, chose  $t_1$  to be the same for all temperatures and all wave vectors. As an illustration, the resulting fits are given, together with the computed functions, in Fig. 5.

Indeed, a stretched exponential describes very well the observed long-time decay at all temperatures. The full set of numerical values for the various parameters are given in Table II for all three wave vectors considered here. It is important to note that at the highest temperatures,  $T > 310 \text{ K}$ , the time decay is so rapid that the results, in particular for the amplitude  $a$ , are somewhat sensitive to the fitting procedure. At low temperatures, on the other hand,  $a$  can be accurately determined but, because the relaxation time is much longer than the simulation time, the stretched-exponential parameters  $\beta$  and  $\tau$  can be extracted only with difficulty. Such uncertainties are indicated by the symbol  $\sim$  in Table II and subsequent ones.

From Table II, it is seen that  $\beta$  increases slightly with decreasing temperature in the range  $275\text{--}305 \text{ K}$ , while for the wave vector dependence at fixed temperature, we observe a slight decrease with increasing  $q$ . No systematic trend can be detected in the neutron-scattering data [12], either in the  $T$  or the  $q$  direction, so that detailed comparisons are difficult. Our  $q$ - $T$ -averaged value of  $\beta$ ,  $0.73$ , nevertheless, is slightly larger than the neutron-scattering value of about  $0.6$ , but agrees better with the specific-heat-thermal-conductivity value of about  $0.75$  (at  $270 \text{ K}$ ) [37]. In view of the simple model we are considering, the somewhat approximate character of the KWW fits, and the large uncertainties in the experimental  $\beta$  values, we conclude that agreement is relatively

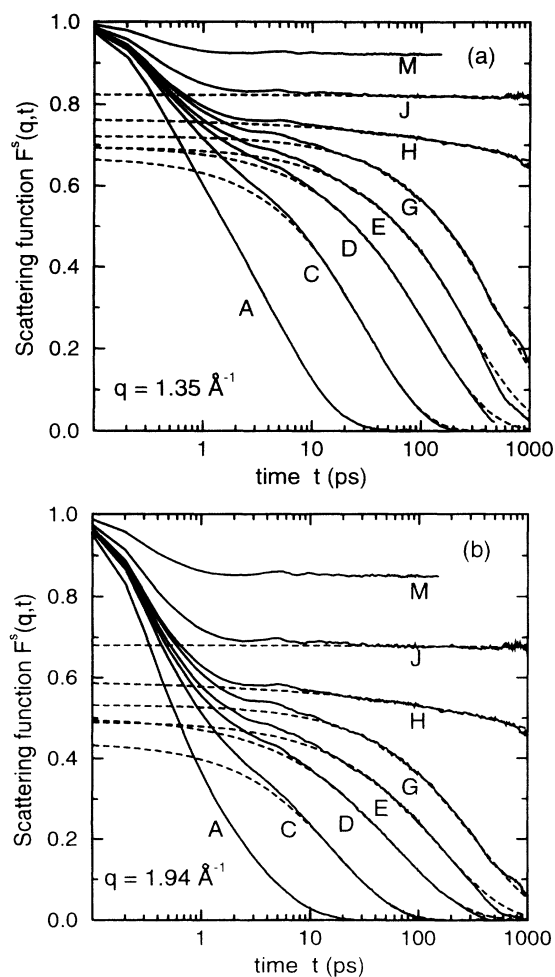


FIG. 5. (a) Self-part of the intermediate scattering function for sites,  $F^s(q, t)$ , vs time, for wave vector  $q = 1.35 \text{ \AA}^{-1}$ , for the various runs discussed in the text, as indicated (cf. Table I); the dashed lines are fits to the KWW expression. (b) Same thing for  $q = 1.94 \text{ \AA}^{-1}$ .

TABLE II. Parameters of the fit to the KWW law, Eq. (3.2), of the self-part of the site-site intermediate scattering function,  $F^s(q, t)$ , for three different values of the wave vector  $q$ ;  $a$  is the amplitude,  $\beta$  is the stretching exponent, and  $\tau$  is the relaxation time. The symbol  $\sim$  indicates that a value is approximate — see text.

Run	$T$ (K)	$q = 1.35$ ( $\text{\AA}^{-1}$ )			$q = 1.94$ ( $\text{\AA}^{-1}$ )			$q = 2.49$ ( $\text{\AA}^{-1}$ )		
		$a$	$\beta$	$\tau$ (ns)	$a$	$\beta$	$\tau$ (ns)	$a$	$\beta$	$\tau$ (ns)
C	318	$\sim 0.671$	$\sim 0.81$	$\sim 0.031$	$\sim 0.440$	$\sim 0.80$	$\sim 0.017$	$\sim 0.283$	$\sim 0.77$	$\sim 0.011$
D	305	0.698	0.73	0.112	0.502	0.67	0.060	0.345	0.62	0.036
E	291	0.695	0.76	0.273	0.492	0.72	0.158	0.332	0.69	0.105
F	281	0.704	0.77	0.264	0.504	0.75	0.149	0.348	0.71	0.097
G	275	0.722	0.80	0.577	0.533	0.77	0.340	0.371	0.75	0.233
H	266	0.767	$\sim 0.35$	$\sim 237$	0.595	$\sim 0.30$	$\sim 132$	0.437	$\sim 0.29$	$\sim 58$
I	255	0.786	$\sim 0.40$	$\sim 119$	0.624	$\sim 0.35$	$\sim 71$	0.472	$\sim 0.32$	$\sim 39$
J	205	0.824			0.681			0.541		
K	173	0.851			0.726			0.604		
L	133	0.896			0.801			0.701		
M	101	0.922			0.850			0.768		

good between model and experiment. Similarly, a detailed comparison of the calculated  $q$  and  $T$ -dependence of the relaxation times with experiment cannot be afforded, but we find  $\tau$  to decrease both with temperature and wave vector, as expected for diffusive motion.

The amplitude parameter  $a \equiv a(q, T)$  for  $\alpha$  processes has often been identified with the “nonergodicity parameter” of MCT, which signals, the presence of a dynamical instability in the system at a “critical temperature”  $T_c$  [4]. Our results for this quantity for site-site correlations are listed in Table II, and also plotted in Fig. 6 for clarity. At low temperatures,  $a(q, T)$  clearly is well described by the corresponding expression for a harmonic Debye system, viz.  $\ln a = -Wq^2T$  (where  $W$  is a constant independent of both  $q$  and  $T$ ), as indicated by dashed lines in Fig. 6. However, for  $T > 250$  K, the system exhibits substantial departure from linearity, i.e., becomes strongly anharmonic;  $a(q, T)$  appears to flatten out for temperatures above 280 K which would correspond, therefore, to the  $T_c$  of MCT.

The physical significance of this non-Debye character of  $a(q, T)$  remains unclear, but very similar behavior has been observed in neutron-scattering measurements of the elastic intensity [12] (equivalent to the nonergodicity parameter), which can also be interpreted in terms of a Debye-Waller factor (or more correctly Lamb-Mössbauer factor),  $S^s(q, \omega \approx 0) \sim \exp(-\langle r^2 \rangle q^2 / 3)$ . In addition to the normal Debye (harmonic) decrease with temperature, the elastic intensity suffers an anomalous (nonharmonic) decrease when approaching a temperature found in the experiments to be located at  $290 \pm 5$  K, in close agreement with our own value for  $T_c$ , and somewhat above the calorimetric  $T_g$ . [The magnitude of  $a(q, T)$  differs, however, but the temperature dependence is entirely similar; again, we do not expect the magnitude to show detailed agreement since our simple model assumes that the neutrons are scattered by the centers of the benzene rings (the sites), rather than the hydrogen nuclei.] Thus, our model appears to reproduce the essential relaxation features seen in the incoherent neutron-scattering studies [12]. In addition, analysis of our data in terms of the dy-

namical susceptibility  $\chi'''(q, \omega) = \omega S^s(q, \omega)$  (Ref. [22]) suggest, consistent with depolarized light scattering experiments [17,38], the existence of a fast process on the time scale 3–20 ps.

We present the above analysis in order to make contact with neutron scattering experiments [12], which also identifies the amplitude of the KWW law with the nonergodicity parameter of MCT; our calculations demonstrate that, to the least, our model is consistent with neutron-scattering data. In order to carry out a detailed test of the predictions of MCT, however, the full time dependence of the scattering function, i.e., over many more decades in time than provided by our MD simulations, should be used. Our simulations are limited to times less

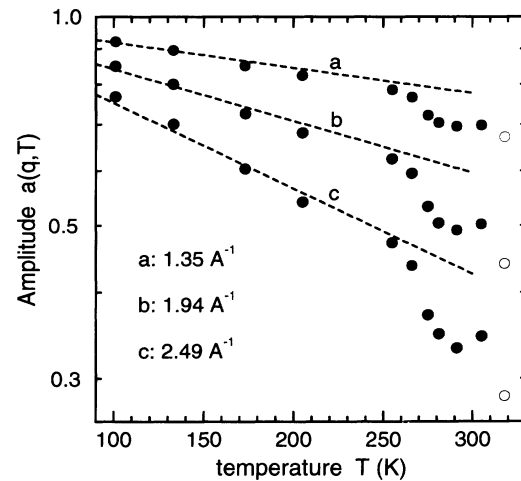


FIG. 6. Amplitude (“nonergodicity parameter”)  $a(q, T)$  vs temperature for the three wave vectors  $q = 1.35, 1.94,$  and  $2.49 \text{ \AA}^{-1}$ . The points at 318 K carry large error bars because of the rapid decay of  $F^s(q, t)$  (cf., e.g., Fig. 5) and the somewhat large and negative pressure (cf. Table I). We show these values by open circles. The dashed lines correspond to the usual linear dependence in the low-temperature harmonic regime.

than  $\sim 1$  ns — much too short for a meaningful and conclusive comparison to be effected since, as noted above, the correlation function at temperatures near  $T_c$  will not decay to zero on this time scale. Neutron-scattering experiments, in fact, face similar problems, while techniques such as light scattering cover a considerably wider frequency (or time) domain (see, e.g., Refs. [19] and [39]), and are thus much more appropriate for putting the MCT to test.

It should be remarked that for temperatures  $T_c=280$  K and below, the calculated intermediate scattering function exhibits substantial decay; only for  $T < 266$  K is a clear plateau observed. The existence of a plateau signals, according to the idealized version of the MCT, the transition of the system to a nonergodic state, and defines  $T_c$ . There are definite uncertainties in our estimate of the critical temperature arising from the fitting procedure, i.e., as we have just seen, our approach might simply be too crude to allow a proper comparison to be carried out. It must be said, also, that processes neglected in the idealized version of the MCT may become important at these temperatures. In the extended version of the MCT, “thermally activated hopping processes” have been incorporated that restore ergodicity below  $T_c$  and influence the long-time decay of the intermediate scattering function around and below  $T_c$ . Whether or not these thermally activated hopping processes have any relation with the actual atomic jump-diffusive events, as observed here in the temperature range 250–270 K (discussed in Sec. III E), is an issue which remains to be resolved.

In summary, while our simulations support the existence of a critical temperature  $T_c$  somewhat above the calorimetric  $T_g$ , consistent with neutron-scattering experiments, they do not, and cannot, because of model limitations (of time, principally), provide a conclusive test of the detailed predictions of the MCT. We note that such a test for *o*-terphenyl was reported recently by Steffen *et al.* using depolarized light scattering [19]. In spite of the large frequency range that was probed (15 decades compared to 6 here), they found it impossible to unambiguously conclude on the validity of MCT.

## 2. Size dependence

The use of periodic boundary conditions may manifest itself in time correlation functions as a local disturbance that can propagate through the system and reappear “at the same place” (*modulo* the periodicity of the system) at a later time, albeit in attenuated form. The time scale for this feedback effect is of the order of  $L/c$ , where  $L$  is the linear size of the periodic cell and  $c$  is the sound velocity. In our case, we find  $L/c \sim 3$  ps with  $L = 50$  Å and using a reasonable sound velocity of  $c = 1500$  m/s [40].

One notes, in Fig. 5, the presence of oscillations on an approximately temperature-independent time scale of a few (about 5) ps. Since this corresponds to the time domain over which the fast relaxation mode is seen in *o*-terphenyl, it is important to assess whether the observed feature is real, or if it arises from our use of a finite MD

simulation cell. We have, therefore, performed a series of runs on a system twice as large in all three directions, i.e., consisting of 2592 molecules (7776 sites). In view of the large size of this new system, only modest runs in time could be afforded, long enough however to cover adequately the time window where the oscillations are visible. The statistical accuracy of the new data, evidently, is inferior to that for the smaller system. The calculated self-intermediate scattering function for sites is displayed in Fig. 7 for a few temperatures, together with the corresponding data for the “normal system.” Indeed, the “first peak” disappears in the large system, but reappears at a time approximately twice as large. We must conclude that the “peak” at about 5 ps is an artifact of our model. Care must, therefore, be taken when interpreting MD time (or frequency) correlation functions on the intermediate time scale.

## 3. Center-of-mass and orientational self-correlations

Our model for *o*-terphenyl is rigid and no intramolecular motion exists. Still, the molecule can rotate and, therefore,  $F^s(q, t)$  contains contributions from both translational and orientational motion. Individual contributions can be isolated by determining the following two functions:

$$F_{c.m.}^s(q, t) = \frac{1}{N} \left\langle \sum_{i=1}^N \exp[i\mathbf{q} \cdot (\mathbf{R}_i^{c.m.}(t) - \mathbf{R}_i^{c.m.}(0))] \right\rangle \quad (3.3)$$

and

$$F_u^s(q, t) = \frac{1}{3N} \left\langle \sum_{i=1}^N \sum_{a=1}^3 \exp[i\mathbf{q} \cdot (\mathbf{u}_{i,a}(t) - \mathbf{u}_{i,a}(0))] \right\rangle, \quad (3.4)$$

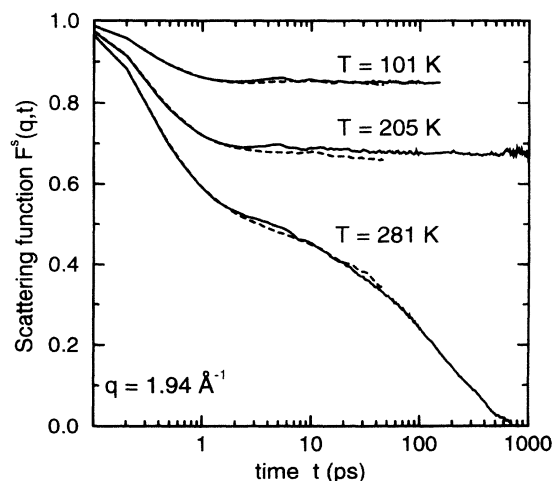


FIG. 7. Self-part of the intermediate scattering function for sites for the 2592-molecule system (dashed lines), compared to the normal-size system (324 molecules — full lines), at the three temperatures indicated, for  $q = 1.94$  Å<sup>-1</sup>.



TABLE III. Parameters of the fit to the KWW law, Eq. (3.2), of the self-part of the intermediate scattering function for centers of mass,  $F_{c.m.}^s(q, t)$ , and orientations,  $F_u^s(q, t)$ , for  $q = 1.94 \text{ \AA}^{-1}$ ;  $a$  is the amplitude,  $\beta$  is the stretching exponent, and  $\tau$  is the relaxation time. The symbol  $\sim$  indicates that a value is approximate — see text.

Run	$T$ (K)	Centers of mass			Orientations		
		$a$	$\beta$	$\tau$ (ns)	$a$	$\beta$	$\tau$ (ns)
C	318	$\sim 0.585$	$\sim 0.87$	$\sim 0.024$	$\sim 0.868$	$\sim 0.59$	$\sim 0.035$
D	305	0.638	0.76	0.080	0.763	0.67	0.151
E	291	0.622	0.84	0.195	0.747	0.75	0.337
F	281	0.644	0.81	0.190	0.756	0.72	0.341
G	275	0.672	0.82	0.420	0.777	0.73	0.743
H	266	0.724	$\sim 0.34$	$\sim 138$	0.789	$\sim 0.53$	$\sim 43.9$
J	205	0.784			0.849		
M	101	0.906			0.935		

which are the analog, for center-of-mass and orientational motion, of the intermediate scattering function  $F^s(q, t)$ . Though these quantities are not available from experiment, they can readily be extracted from our simulations, and will be used as probes in order to determine individual contributions to relaxation.

Just as with  $F^s(q, t)$ , we have fitted the center-of-mass and orientational functions to the KWW law, Eq. (3.2); as an illustration, we give in Table III the results for wave vector  $q = 1.94 \text{ \AA}^{-1}$ . The qualitative behavior of  $F_{c.m.}^s(q, t)$  and  $F_u^s(q, t)$ , we find, is very much the same as that of  $F^s(q, t)$ . This indicates that, at least in the range of temperatures investigated, translational and rotational motions are strongly coupled, so that the structural changes that take place during  $\alpha$  relaxation must involve both types of motion.

Quantitatively, there are only small differences between the various scattering functions. The orientational correlation function shows somewhat more stretching than the correlation function for centers of mass,  $\beta_u = 0.72$  vs  $\beta_{c.m.} = 0.81$ , where  $\beta$  is the average value for the exponent  $\beta$  in the stretched exponential (utilizing only the “reliable” values). The corresponding value for site-site correlations is  $\bar{\beta} = 0.73$ , i.e., very similar to that for orientational motion. This would indicate that center-of-mass motion is more liquidlike than orientational motion ( $\beta = 1$  in a simple liquid). The temperature dependence of the relaxation time  $\tau$ , on the other hand, is found to be quite similar for site and center-of-mass dynamics, with the  $\alpha$  relaxation slower for orientational motion.

We have tried to determine whether the large anharmonicity seen in the nonergodicity parameter for sites, Fig. 6, is mainly caused by center-of-mass or by orientational motion. We find, by considering the values of the amplitudes in Table III, that both kinds of motion behave in a comparable way. We conclude, therefore, in line with the above discussion, that the observed anharmonic behavior on approaching  $T_c$  cannot be characterized as either primarily orientational or primarily translational.

#### 4. Total intermediate scattering function

In order to assess the relative importance of self-(incoherent) contributions to the full scattered intensity,

we have calculated the *total* intermediate scattering function  $F(q, t)$  for sites, defined in Eq. (3.1). The evolution in temperature of this function, normalized with respect to its initial value,  $F(q, t)/F(q, 0)$ , for the case  $q = 1.94 \text{ \AA}^{-1}$ , is displayed in Fig. 8. This should be compared with the corresponding data in the case of self-correlations, Fig. 5(b). Evidently, the behavior of the two functions are very similar, which indicates that the dynamics is dominated, at this wave vector, by the single-particle motion. Indeed, we have fitted, again, the calculated functions to the KWW expression; the resulting parameters are presented in Table IV. The values for  $\beta$  and  $\tau$  are quite similar to those for self-correlations, Table II, while the values for  $a$  are quite different, reflecting the fact that  $a$ , basically a form factor [4], includes information on structural aspects, which differ for self- and total parts.

#### E. Self-part of the van-Hove correlation function

We now examine the molecular origin of the mesoscopic relaxation phenomenon in real space. A detailed

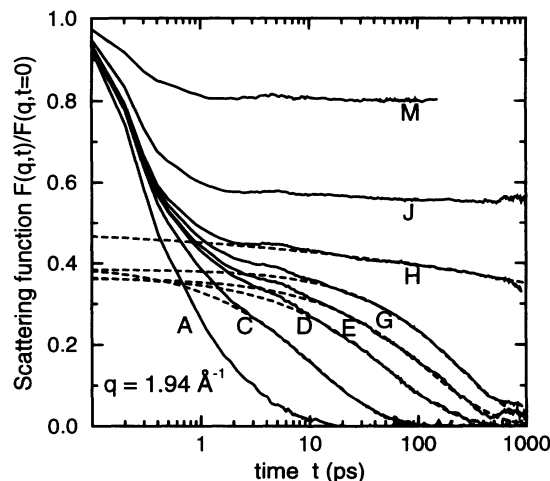


FIG. 8. Total intermediate scattering function for sites normalized to unity at  $t=0$ ,  $F(q, t)/F(q, t=0)$ , vs time, for wave vector  $q = 1.94 \text{ \AA}^{-1}$ , for the various runs discussed (cf. Table I); the dashed lines are fits to the KWW expression.

TABLE IV. Parameters of the fit to the KWW law, Eq. (3.2), of the total site-site intermediate scattering function,  $F(q, t)$ , for  $q = 1.94 \text{ \AA}^{-1}$ ;  $a$  is the amplitude,  $\beta$  is the stretching exponent, and  $\tau$  is the relaxation time. The symbol  $\sim$  indicates that a value is approximate — see text.

Run	$T$ (K)	$a$	$\beta$	$\tau$ (ns)
C	318	$\sim 0.395$	$\sim 0.69$	$\sim 0.012$
D	305	0.369	0.68	0.055
E	291	0.364	0.71	0.129
F	281	0.371	0.80	0.132
G	275	0.385	0.77	0.246
H	266	0.500	$\sim 0.17$	$\sim 328$
J	205	0.577		
M	101	0.800		

picture of single-particle motion is provided by the van-Hove self-correlation function [36],

$$G^s(r, t) = \frac{1}{3N} \left\langle \sum_{i=1}^N \sum_{\alpha=1}^3 \delta[\mathbf{r} - (\mathbf{R}_{i,\alpha}(t) - \mathbf{R}_{i,\alpha}(0))] \right\rangle, \quad (3.5)$$

the spatial Fourier transform of the self-intermediate scattering function. This function, multiplied by  $4\pi r^2 G^s(r, t)$ , is plotted in Fig. 9 at three temperatures, namely 291 K (in the liquid phase), 275 K (close to  $T_c$ ), and 266 K (well into the supercooled regime), and for different times in the range 1–1000 ps. At each temperature, the function has a single peak which moves to larger distances with increasing time; at the lowest temperature, this motion is essentially arrested (on the time scale of our simulations) at about 0.7  $\text{\AA}$ .

In a previous publication [21], we have demonstrated that the van Hove self-correlation function shows a strong non-Gaussian spatial dependence at intermediate times. To emphasize this effect, we have included, as dashed lines in Fig. 9, the Gaussian function  $(2\pi)^{-1/2} (2r^2/r_G^3) \exp(-r^2/2r_G^2)$ , where the width  $r_G$  is determined by fitting to short distances for  $t = 100$  ps. The non-Gaussian character of the van-Hove function is evident. It can in fact be quantified in terms of an average “non-Gaussian” parameter; we have done this in Ref. [21], and find, in addition to strong deviations from Gaussian behavior, that comparatively few particles undergo large anharmonic motion.

There is no clear sign, at any temperature, of the ubiquitous two-peak structure found in simple atomic models in the supercooled regime [26,41]. The occurrence of a second peak in atomic glasses is the clear signature of jump-diffusive motion with one or several particles involved. Clearly, the added complexity of molecular — as opposed to atomic — entities is sufficient to inhibit jump diffusion, at least on the ns time scale under consideration here. Note, however, that there is nevertheless some processes taking place at low temperatures, below  $T_c$ . This can be inferred in Fig. 9(c) (at  $T = 266$  K) from the extremely small contributions that develop at long times for distances larger than nearest neighbor. We stress this by multiplying by ten the tail of the  $t = 1000$  ps func-

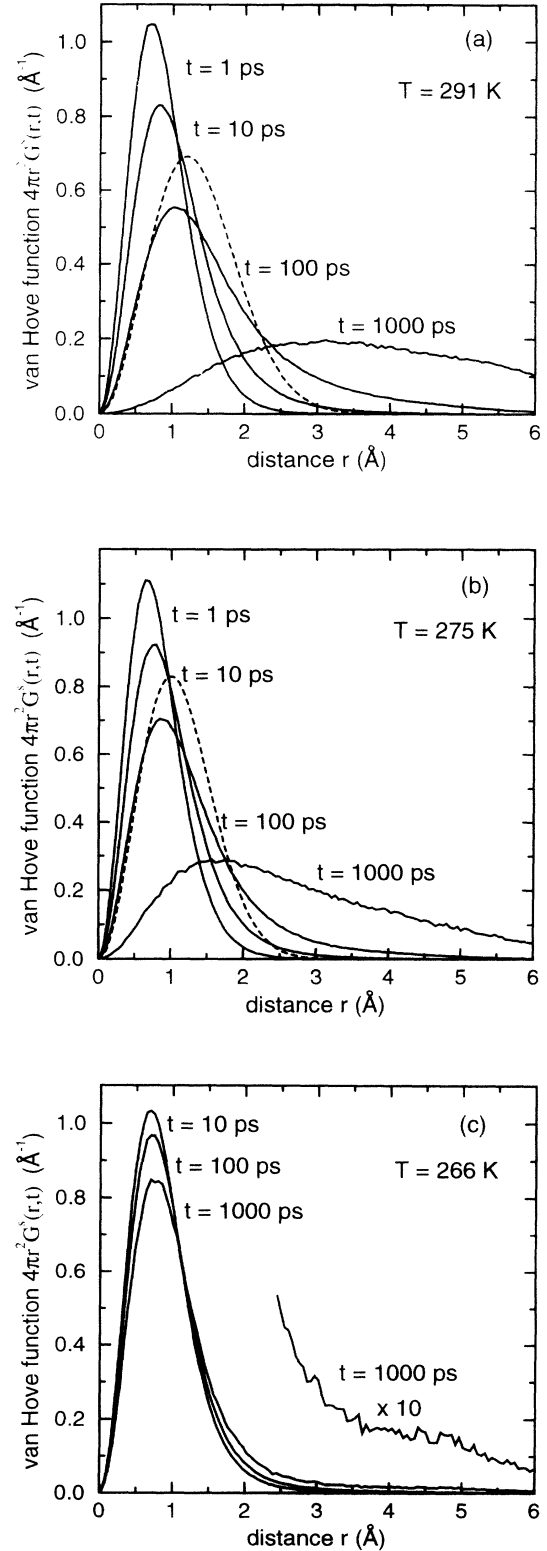


FIG. 9. (a) Self-part of the van-Hove correlation function  $G^s(r, t)$  multiplied by  $4\pi r^2$ , at  $T = 291$  K, for four different times, as indicated; the dashed curve is a Gaussian function whose width was determined by fitting the  $t = 100$  ps function at short distances (see text). (b) Same thing, but at  $T = 275$  K. (c) The same function at  $T = 266$  K for times 10, 100, and 1000 ps.

tion. This should be contrasted with the corresponding function for center-of-mass motion,  $G_{\text{c.m.}}^s(r, t)$ , shown in Fig. 10 (for the same temperature of 266 K), which goes to zero more rapidly. The difference between  $G_{\text{c.m.}}^s(r, t)$  and  $G^s(r, t)$ , therefore, must come from the motion of the molecules *about* their centers of mass, i.e., reorientations. In fact, direct observation of the orientational trajectories of the molecules reveal the existence, even at such low temperatures, of a number of “two-level system” reorientations of the molecules in the near absence of center-of-mass motion, corresponding to the strongly hindered motion of molecules temporarily trapped in the cage formed by surrounding molecules; these results are presented in Ref. [23]. The small differences between center-of-mass and orientational motion at low temperatures (266 K) are most clearly revealed by the van-Hove correlation function, even though they are in principle present in the time dependence of the intermediate scattering function.

It has been observed, as already mentioned in the introduction, that rotational and translational motion “decouple” below  $T_c$  [16]; our results, however, suggest more the opposite conclusion; translational motion becomes slower compared with rotational motion. However, our simulation can only provide data in the ns time region and we, therefore, cannot say anything about the dynamics on longer time scale.

To reveal the strictly orientational motion in more detail, we have determined the average time-dependence of the orientation in space of the molecules. We introduce, for this purpose, the angles  $\theta_i^a(t)$  defined by

$$\theta_i^a(t) = \cos^{-1}[(\mathbf{u}_i^a(t) \cdot \mathbf{u}_i^a(0))/(\mathbf{u}_i^a(0) \cdot \mathbf{u}_i^a(0))], \quad (3.6)$$

where  $\mathbf{u}_i^a$  is defined in Eq. (2.1), and examine the distributions of these angles,

$$P^a(\theta, t) = \frac{1}{N} \left\langle \sum_{i=1}^N \delta[\theta - \theta_i^a(t)] \right\rangle. \quad (3.7)$$

We show, in Fig. 11, the evolution in time of the tail of the distributions at a temperature of 266 K; Fig. 11(a)

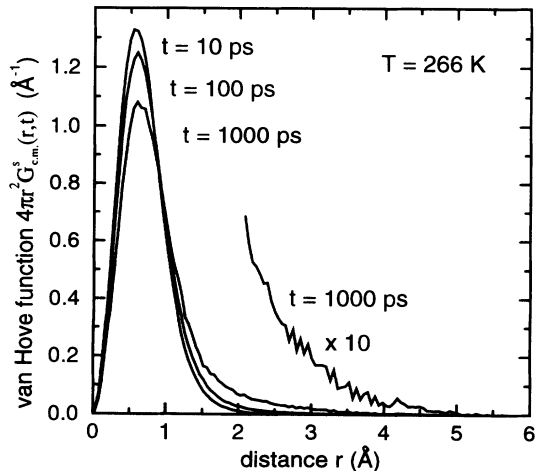


FIG. 10. Same as Fig. 9(c), but for centers of mass.

is for the middle site of the molecule, while Fig. 11(b) corresponds to the average of the two end sites. At short times,  $P(\theta, t)$  is strongly peaked around  $\theta=0$ ; at sufficiently long times, if the orientation of a molecule is uncorrelated to its initial value, as is the case in a liquid,  $P(\theta, t)$  would approach  $\sin(\theta)/2$ . The former is more or less the case here, as the system is essentially frozen on the time scale of the simulation. We find here that a minute — but nevertheless clear — “second” peak develops at long times (close to about  $90^\circ$ ), particularly evident for the middle site. This is a direct manifestation of the existence of jumplike reorientations of the molecules, analog to translational jump diffusion in atomic systems at low temperature. Thus, even at low temperatures, some motion is taking place on the ns time scale that cannot be characterized as simple vibrational motion.

#### IV. SUMMARY AND CONCLUSIONS

Molecular-dynamics simulations have been used to study relaxation in the van der Waals glass-former *o*-

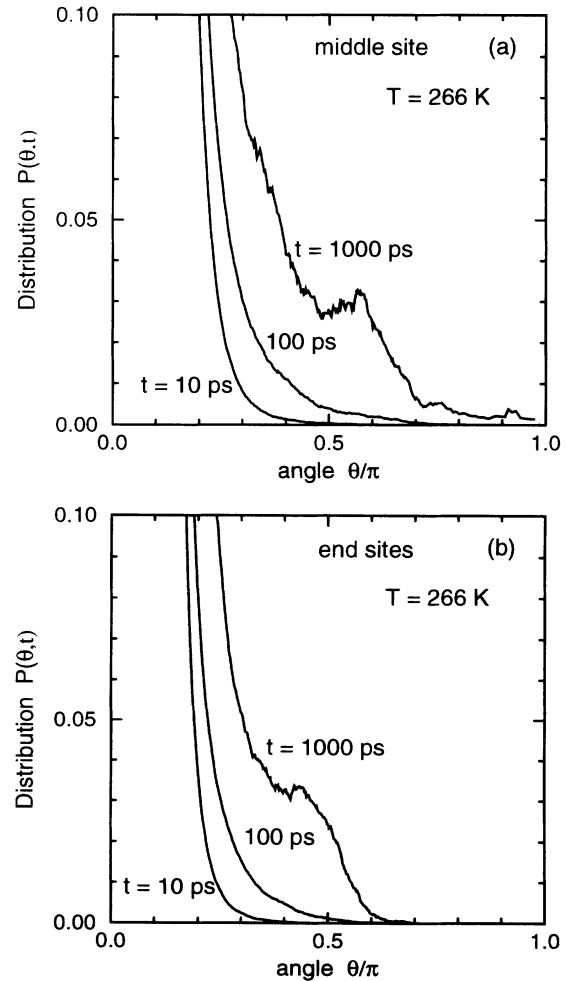


FIG. 11. Distribution  $P(\theta, t)$  of the orientation angles defined in the text, at  $T = 266$  K, for three different times, for (a) the middle site, and (b) the two end sites (averaged).

terphenyl. The molecule was treated as a rigid three-site complex, each site playing the role of a whole benzene ring, so that intramolecular motion was not taken into account. A total of 14 different temperatures were investigated in the range  $100 \text{ K} < T < 400 \text{ K}$ , with the longest ones extending in time to a few ns.

In order to characterize the relaxation processes, we have focused our attention on the intermediate scattering function  $F^s(q, t)$ , also accessible in neutron-scattering measurements, and its real-space Fourier transform, the van-Hove self-correlation function  $G^s(r, t)$ , which provides a detailed picture of the microscopic motion. Our results may be summarized as follows:

(i) At high temperatures,  $320 \text{ K} < T < 400 \text{ K}$ , the system behaves more or less as an ordinary liquid, with the diffusion coefficient for centers of mass  $D_{\text{c.m.}}$  ranging from  $60 \times 10^{-7}$  down to about  $10 \times 10^{-7} \text{ cm}^2 \text{ s}^{-1}$ .

(ii) At lower temperatures,  $270 \text{ K} < T < 320 \text{ K}$ , the relaxation slows down considerably and we find that the long-time decay is well described by a Kohlrausch law. The zero-time amplitude of this process, the “nonergodicity parameter” of the mode-coupling theory, which can also be interpreted as a Debye-Waller factor, is seen to depart from a harmonic (linear) temperature dependence and exhibit a “singular” behavior at about  $T_c = 280 \text{ K}$ , a temperature substantially larger than the conventional glass transition temperature  $T_g = 243 \text{ K}$ . This result correlates well with neutron-scattering data [12], as well as with the predictions of mode-coupling theory [4], though statistical limitations do not allow a precise comparison to be carried out. We find, additionally, that the observed anharmonic behavior around  $T_c$ , as well as the decay of the scattering functions, is equally evident from both orientational and translational correlations. The latter observation indicates that the structural changes that take place during  $\alpha$  relaxation are neither specifically orientational nor specifically translational.

The van-Hove self-correlation function  $G^s(r, t)$  exhibits, at these temperatures, a strong non-Gaussian spatial dependence at intermediate and long times and we find in addition that comparatively few molecules make large contributions to this motion [21]. In contrast to the case of simple atomic systems [26,41], we see no sign in  $G^s(r, t)$  of the two-peak feature that is a signature of

jump-diffusive motion.

(iii) At slightly lower temperatures,  $250 \text{ K} < T < 270 \text{ K}$ , the system is essentially frozen. However, some relaxation is still visible in  $F^s(q, t)$  and close inspection of  $G^s(r, t)$ , as well as of the molecules angular distribution functions, reveals that processes are taking place that cannot be described as simple vibrational motion. It is found, in fact, that several molecules undergo rapid reorientations in the cage formed by the surrounding molecules, in the near-absence of center-of-mass motion [23].

It has been observed that, below  $T_c$ , translational and rotational motion “decouple,” the rotational motion becoming comparatively slower [16]. Our data suggest more the opposite behavior; the translational motion becomes slower compared with the rotational motion, but it should be kept in mind that the present simulations can only probe the dynamics of the system on the ns time scale. In the temperature range of relevance here (250–270 K), the diffusion coefficient cannot be determined from the simulation. Only values down to about  $10^{-7} \text{ cm}^2 \text{ s}^{-1}$  can be extracted with some confidence from the data, which are several orders of magnitude larger than the relevant experimental values.

(iv) At even lower temperatures,  $T < 250 \text{ K}$ ,  $F^s(q, t)$  decays to a constant value, the “nonergodicity” parameter, within a few ps. The system vibrates essentially harmonically, as deduced from the temperature dependence of that parameter.

## ACKNOWLEDGMENTS

This work was supported by grants from the Natural Science and Engineering Research Council (NSERC) of Canada and the “Fonds pour la formation de chercheurs et l’aide à la recherche” of the Province of Québec to L.J.L., as well as by the Swedish Natural Science Research Council (NFR) to G.W. The calculations reported here were performed on the Cray Y-MP/C-90 at the Pittsburgh Supercomputer Center thanks to a grant allocated to L.J.L. by the “Services informatiques de l’Université de Montréal.”

- 
- [1] See for instance S.R. Elliott, *Physics of Amorphous Materials* (Longman, London, 1983); or J. Jäckle, *Rep. Prog. Phys.* **49**, 171 (1986).
- [2] M.H. Cohen and G.S. Grest, *Phys. Rev. B* **24**, 4091 (1981).
- [3] E. Leutheusser, *Phys. Rev. A* **29**, 2765 (1984); U. Bengtzelius, W. Götze, and A. Sjölander, *J. Phys. C* **17**, 5915 (1984); T.R. Kirkpatrick, *Phys. Rev. A* **31**, 939 (1985); S.P. Das, G.F. Mazenko, S. Ramaswamy, and J. Toner, *Phys. Rev. Lett.* **54**, 118 (1985).
- [4] For a recent review, see W. Götze and L. Sjögren, *Rep. Prog. Phys.* **55**, 241 (1992).
- [5] S.P. Das and G.F. Mazenko, *Phys. Rev. A* **34**, 2265 (1986); S.P. Das, *ibid.* **36**, 211 (1987); B. Kim and G.F. Mazenko, *Adv. Chem. Phys.* **78**, 129 (1990).
- [6] W. Götze and L. Sjögren, *Z. Phys. B* **65**, 415 (1987); *J. Phys. C* **21**, 3407 (1988); L. Sjögren, *Z. Phys. B* **79**, 5 (1990).
- [7] R. Schmitz, J.W. Dufty, and P. De, *Phys. Rev. Lett.* **71**, 2066 (1993).
- [8] C.A. Angell, *J. Phys. Chem. Solids* **49**, 863 (1988).
- [9] R.J. Greet and D. Turnbull, *J. Chem. Phys.* **46**, 1243 (1967).
- [10] G.P. Johari and M. Goldstein, *J. Chem. Phys.* **53**, 2372 (1970).
- [11] L. Wu and S.R. Nagel, *Phys. Rev. B* **46**, 11 198 (1992).
- [12] E. Bartsch, F. Fujara, M. Kiebel, H. Sillescu, and W. Petry, *Ber. Bunsenges. Phys. Chem.* **93**, 1252 (1989).

- [13] O. Debus, H. Zimmermann, E. Bartsch, F. Fujara, M. Kiebel, W. Petry, and H. Sillescu, *Chem. Phys. Lett.* **180**, 271 (1991).
- [14] W. Petry, E. Bartsch, F. Fujara, M. Kiebel, H. Sillescu, and B. Farago, *Z. Phys. B* **83**, 175 (1991); E. Bartsch, O. Debus, F. Fujara, M. Kiebel, W. Petry, and H. Sillescu, *Ber. Bunsenges. Phys. Chem.* **95**, 1146 (1991).
- [15] M. Kiebel, E. Bartsch, O. Debus, F. Fujara, W. Petry, and H. Sillescu, *Phys. Rev. B* **45**, 10 301 (1992).
- [16] F. Fujara, B. Geil, H. Sillescu, and G. Fleischer, *Z. Phys. B* **88**, 195 (1992).
- [17] E.W. Fischer, G. Meier, T. Rabenau, A. Patkowski, W. Steffen, and W. Thönnies, *J. Non-Crystall. Solids* **131-133**, 134 (1991); E.W. Fischer, E. Donth, and W. Steffen, *Phys. Rev. Lett.* **68**, 2344 (1992); W. Steffen, A. Patkowski, G. Meier, and E.W. Fischer, *J. Chem. Phys.* **96**, 4171 (1992).
- [18] W. Schnauss, F. Fujara, and H. Sillescu, *J. Chem. Phys.* **97**, 1378 (1992).
- [19] W. Steffen, A. Patkowski, H. Gläser, G. Meier, and E.W. Fischer, *Phys. Rev. E* **49**, 2992 (1994).
- [20] For a review of the MD technique, see M.P. Allen and D.J. Tildesley, *Computer Simulation of Liquids* (Clarendon, Oxford, 1987).
- [21] L.J. Lewis and G. Wahnström, *Solid State Commun.* **86**, 295 (1993).
- [22] G. Wahnström and L.J. Lewis, *Physica A* **201**, 150 (1993).
- [23] L.J. Lewis and G. Wahnström, *Proceedings of the Second International Discussion Meeting on Relaxations in Complex Systems*, edited by K.L. Ngai, E. Riande, and G.B. Wright, *J. Non-Cryst. Solids* **172-174**, 69 (1994).
- [24] For a review, see J.-L. Barrat and M.L. Klein, *Annu. Rev. Phys. Chem.* **42**, 23 (1991); Y. Hiwatari, H. Miyagawa, and T. Odagaki, *Solid State Ionics* **47**, 179 (1991).
- [25] H. Miyagawa, Y. Hiwatari, B. Bernu, and J.-P. Hansen, *J. Chem. Phys.* **88**, 3879 (1988).
- [26] G. Wahnström, *Phys. Rev. A* **44**, 3752 (1991).
- [27] G.F. Signorini, J.-L. Barrat, and M.L. Klein, *J. Chem. Phys.* **92**, 1294 (1990).
- [28] P. Sindzingre and M.L. Klein, *J. Chem. Phys.* **96**, 4681 (1992).
- [29] J. Alonso, F.J. Bermejo, M. García-Hernández, J.L. Martínez and W.S. Howells, *J. Mol. Struct.* **250**, 147 (1991); J. Alonso, F.J. Bermejo, M. García-Hernández, J.L. Martínez, W.S. Howells, and A. Criado, *J. Chem. Phys.* **96**, 7696 (1992); F.J. Bermejo, J. Alonso, A. Criado, F.J. Mompeán, J.L. Martínez, M. García-Hernández, and A. Chahid, *Phys. Rev. B* **46**, 6173 (1992).
- [30] Th. Dries, F. Fujara, M. Kiebel, E. Rössler, and H. Sillescu, *J. Chem. Phys.* **88**, 2139 (1988); **90**, 7613(E) (1989).
- [31] C.J. Birkett Clews and K. Lonsdale, *Proc. R. Soc. London Ser. A* **161**, 493 (1937).
- [32] S. Aikawa and Y. Maruyama, *Acta Crystallogr. B* **34**, 2901 (1978).
- [33] J. Opdycke, J.P. Dawson, R.K. Clark, M. Dutton, J.J. Ewing, and H.H. Schmidt, *J. Phys. Chem.* **68**, 2385 (1964).
- [34] D.W. McCall, D.C. Douglass, and D.R. Falcone, *J. Chem. Phys.* **50**, 3839 (1969).
- [35] E. Bartsch, H. Bertagnolli, P. Chieux, A. David, and H. Sillescu, *Chem. Phys.* **169**, 373 (1993).
- [36] See, for instance, J.-P. Hansen and I.R. McDonald, *Theory of Simple Liquids* (Academic, London, 1986).
- [37] P.K. Dixon and S.R. Nagel, *Phys. Rev. Lett.* **61**, 341 (1988).
- [38] L. Börjesson and A.K. Hassan (unpublished).
- [39] H.Z. Cummins, W.M. Du, M. Fuchs, W. Götze, S. Hildebrand, A. Latz, G. Li, and N.J. Tao, *Phys. Rev. E* **47**, 4223 (1993).
- [40] G. D'Arrigo, *J. Chem. Phys.* **63**, 61 (1975).
- [41] J.-L. Barrat, J.-N. Roux, and J.-P. Hansen, *Chem. Phys.* **149**, 197 (1990).